METHOD

Journal of Anatomy ANATOMICAL SOCIETY WILEY

ArUco-based stylus reliability for reproductible 3D digitalisation of shoulder cartilage contours

Florent Moissenet[1,2] 🔸 | Christian Elmo Kulanesan[3] 🔸 | Kevin Co[4] | Pablo Rodriguez[5] |
Pierre Vacher[3] | Jean-Yves Beaulieu[6] | Nicolas Holzer[1,5]

[1]Biomechanics Laboratory, Geneva
University Hospitals and University of
Geneva, Geneva, Switzerland

[2]Kinesiology Laboratory, Geneva
University Hospitals and University of
Geneva, Geneva, Switzerland

[3]Université Savoie Mont Blanc Laboratoire
SYMME, Annecy-le-Vieux, France

[4]Laboratory of Simulation and Movement
Modeling, School of Kinesiology and
Exercise Sciences, Université de Montréal,
Montreal, Quebec, Canada

[5]Department of Surgery, Geneva
University Hospitals, Geneva, Switzerland

[6]Department of Anatomy, Faculty of
Medicine, University of Geneva, Geneva,
Switzerland

Correspondence
Florent Moissenet, Biomechanics
Laboratory, Geneva University Hospitals
and University of Geneva, Geneva,
Switzerland.
Email: florent.moissenet@unige.ch

Abstract

Imaging techniques in anatomy have developed rapidly over the last decades through the emergence of various 3D scanning systems. Depending on the dissection level, non-contact or tactile contact methods can be applied on the targeted structure. The aim of this study was to assess the inter and intra-observer reproducibility of an ArUco-based localisation stylus, that is, a manual technique on a hand-held stylus. Ten fresh–frozen, unembalmed adult arms were used to digitalise the glenoid cartilage related to the glenohumeral joint and the contour of the clavicle cartilage related to the acromioclavicular joint. Three operators performed consecutive digitalisations of each cartilage contour using an ArUco-based localisation stylus recorded by a single monocular camera. The shape of each cartilage was defined by nine shape parameters. Intra-observer repeatability and inter-observer reproducibility were computed using an intra-class correlation (ICC) for each of these parameters. Overall, 35.2 ± 2.4 s and 26.6 ± 10.2 s were required by each examiner to digitalise the contour of a glenoid and acromioclavicular cartilage, respectively. For most parameters, good-to-excellent agreements were observed concerning intra-observer (ICC ranging between 0.81 and 1.00) and inter-observer (ICC ranging between 0.75 and 0.99) reproducibility. To conclude, through a fast and versatile process, the use of an ArUco-based localisation stylus can be a reliable low-cost alternative to conventional imaging methods to digitalise shoulder cartilage contours.

KEYWORDS
3D digitalisation, ArUco markers, cartilage, hand-held stylus, shoulder

1 | INTRODUCTION

Imaging techniques in anatomy have developed rapidly over the last decades through the emergence of various 3D scanning systems (Sindhu & Soundarapandian, 2019). Depending on the dissection level, non-contact or tactile contact methods can be applied on the targeted structure (Sindhu & Soundarapandian, 2019). On one hand, non-contact methods are widely represented by

medical imaging techniques (e.g., CT, MRI, x-rays, and ultrasound) (Haleem & Javaid, 2019), as well as surface scanning techniques (e.g., time of flight, laser, and structured lighting) (Sood et al., 2021). On the other hand, tactile contact methods can be based on automatic techniques such as coordinate measuring machine and robotic arms (Sindhu & Soundarapandian, 2019) or manual techniques often based on a hand-held stylus (Hargett et al., 2020). This last category offers a versatile approach to

scan structures using any tracking system and allows 3D scanning at reduced cost.

Recent developments in vision introduced new approaches for optical tracking based on binary square fiducial markers. Garrido-Jurado et al. (2014) suggested highly reliable fiducial markers called ArUco markers. On this basis, several authors proposed to combine multiple ArUco markers to define a hand-held stylus (Le et al., 2022). Their studies demonstrated that this approach could lead to a sub-millimetric accuracy (0.4 mm at 60 Hz over a 30×40 cm with a 2.1 Mpx camera) working area tracking with a low-cost system based on a simple 2D camera based on monocular vision. Still, to the best of our knowledge, the reliability of an ArUco-based localisation stylus remains unknown. Such an assessment is yet required to estimate the measurement error of this instrument and its reproducibility across examiners.

The aim of this study was to assess the inter and intra-observer reproducibility of an ArUco-based localisation stylus. This was tested during the 3D digitalisation of shoulder cartilage contours. To do so, three operators digitalised the contour of the glenoid cartilage related to the glenohumeral joint and the contour of the clavicle cartilage related to the acromioclavicular joint. It was hypothesised that the use of the ArUco-based localisation stylus allows for the 3D digitalisation of cartilage contours, or other anatomical structures, in a simple, versatile, and reliable process.

2 | METHODS

2.1 | Specimen preparation

The sample size required for this study was computed using the *ICC.Sample.Size* R package (v. 1.0) (R-Core-Team, 2020a) (R 4.1.2 and RStudio version 2021.09.0 build 351) where intra-class correlation (ICC) was defined as the primary outcome (see Section 2.5). Based on previous experiments involving ex vivo knee ligament attachments digitalised with a hand-held stylus (Athwal et al., 2020), the hypothesised ICC value was set to 0.9. The resulting requested sample size was $N=8$. To anticipate potential dropouts, 10 fresh–frozen, unembalmed adult arms (five right sides and five left sides) were obtained from a previous study (Moissenet et al., 2022). None of the limbs had an advanced degenerative joint disease or previous ligamentous injury confirmed by direct inspection and radiographs before experiments. All pieces were acquired at the Anatomy Teaching Unit of the Geneva Faculty of Medicine. They were all selected from the local body donation programme. The Cantonal Commission for Research Ethics approved this study (2020-00598). All procedures were performed in accordance with ethical standards of the institutional research committee and with the 1964 Helsinki Declaration and later amendments.

All pieces were stored at −20° and thawed at room temperature during approximately 72 h prior to testing. Dissection of the pieces consisted in resecting all the soft parts to preserve only bones and cartilage. An anatomical set of 10 dissected scapulas and clavicles was then used in this study.

2.2 | Cartilage contour digitalisation

Cartilage contours were digitalised using an ArUco-based localisation stylus (Figure 1). The 3D localisation of the stylus tip (1-mm radius spherical contact probe) was made available using a set of planar ArUco markers (Garrido-Jurado et al., 2014) glued on the surface of a double dodecahedron secured at an the other extremity of the stylus.

The position of ArUco markers was recorded by a 3.1-Mpx monocular camera (EXO252 MU3, SVS-Vistek, Germany) equipped with a 12-mm focus camera zoom length (PENTAX TV, PENTAX, Japan) at each motion frame (10 Hz). After a preliminary calibration phase, the 3D position of each marker and of the stylus tip was stored in the stylus reference coordinate system, arbitrarily defined
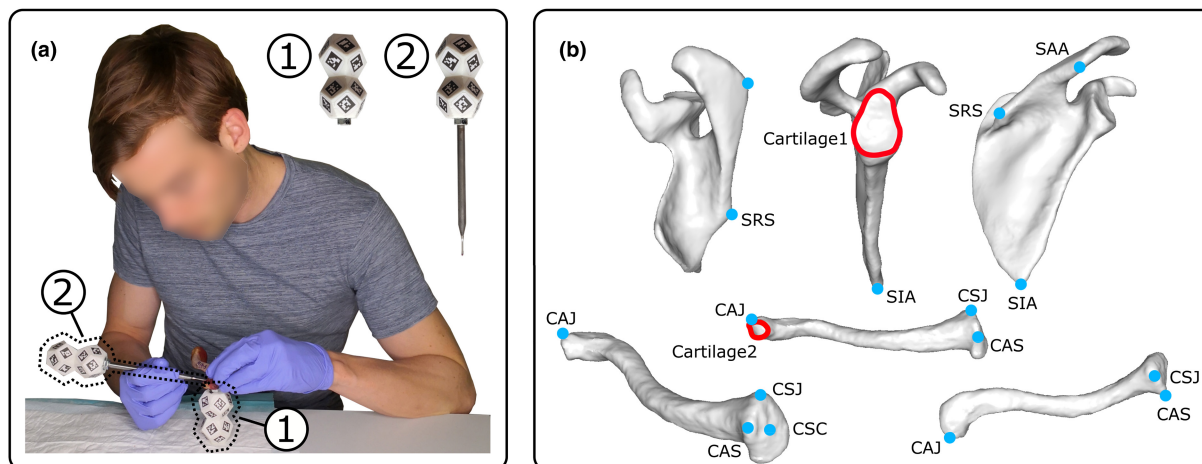

FIGURE 1 Cartilage contour digitalisation procedure. (a) Use of a stylus (2), equipped with ArUco markers on a double dodecahedron, to digitalise anatomical landmarks and cartilage contours. The bone is also instrumented with a double dodecahedron with ArUco markers (1). (b) Illustration of the digitalised anatomical landmarks and cartilage contours (see Table 1 for details). The nomenclature used for anatomical landmarks is based on the propositions made by Van Sint Jan (2007).

TABLE 1 Digitalised anatomical landmarks and cartilage contours. The nomenclature used for anatomical landmarks is based on the propositions made by Van Sint Jan (2007).

Type	Bone	ID	Description
Anatomical landmarks	Scapula	SIA	Most distal point of the scapula lower angle
		SRS	Lateral point of the spine base triangle
		SAA	Acromial angle
	Clavicle	CAJ	Superior edge centre of the acromioclavicular joint on the clavicle
		CSJ	Superior edge centre of the sternoclavicular joint on the clavicle
		CAS	Anterior border apex of the sternoclavicular joint on the clavicle
		CSC	Centre of the sternoclavicular cartilage on the clavicle
Cartilage contours	Scapula	Cartilage1	Contour of the glenoid cartilage related to the glenohumeral joint
	Clavicle	Cartilage2	Contour of the clavicle cartilage related to the acromioclavicular joint

(Wu et al., 2017). A double dodecahedron was used in this study to avoid coplanarity (Schweighofer & Pinz, 2006). In such conditions, the stylus tip can be located irrespective of its position with a standard deviation of 0.3 mm along the camera optical axis and 0.1 mm along the two perpendicular axes (Elmo Kulanesan, 2023). For that, at least two ArUco markers must be visible by the camera, with sufficient depth of field and negligible motion blur.

The digitalisation process was performed sequentially. First, a set of anatomical landmarks (Figure 1; Table 1) were pointed by one examiner (PR) to define bone coordinate systems (see Section 2.3). Second, the contour of the glenoid cartilage related to the glenohumeral joint and the contour of the clavicle cartilage related to the acromioclavicular joint were digitalised. This choice was guided by temporal constraints and to assess cartilages with different sizes and shapes. To assess the inter and intra-observer reliability of this digitalisation procedure, three examiners (PR, CE, and FM) performed three consecutive digitalisations of each cartilage contour.

2.3 | Bone coordinate systems

To allow comparison between digitalisations, the 3D point clouds defining each cartilage contour were expressed in a bone coordinate system (orthonormal coordinate system: X_b, Y_b, Z_b) (Figure 2). This coordinate system was defined using the previously defined anatomical landmarks following the recommendations of the International Society of Biomechanics (ISB) (Wu et al., 2005). Only X_c^b of the clavicle was defined using another approach, as the thorax, needed in ISB recommendations, was not available is this study. For that, the centre of the sternoclavicular joint was used in combination with the anterior border apex of this joint to define the clavicle antero-posterior axis. This procedure is similar to the one previously proposed by Gutierrez Delgado et al. (2017). To record the position and orientation of the bone coordinate system, each bone was also instrumented with a double dodecahedron made of ArUco markers (Figure 1).

2.4 | Position, orientation, and shape of the cartilage contour

Firstly, the cartilage contour 3D point cloud (expressed in the related bone coordinate system) was projected orthogonally on its least-squares plane (Figure 3a). The resulting 2D point cloud was fitted with an ellipse using a least-squares approach based on orthogonal distance (Dingler, 2021) (Figure 3b). An ellipse coordinate system (orthonormal coordinate system: X_e, Y_e, Z_e), centred on the resulting ellipse centre, was defined using three unit vectors: along the ellipse major axis, along the ellipse minor axis, and along the least-squares plane normal vector pointing laterally (Figure 3a). Secondly, the cartilage 3D point cloud contour was projected orthogonally on a plane having as the normal vector the previously defined unit vector along the ellipse minor axis (Figure 3c). The resulting 2D point cloud was fitted with a least-squares circle (Figure 3a).

A cartilage contour was thus defined by nine parameters. Six parameters were used to describe its 3D position (**T**: $X_{cart}, Y_{cart}, Z_{cart}$) and orientation (**R**: $\alpha_{cart}, \beta_{cart}, \gamma_{cart}$) in the bone coordinate system. Three other parameters were used to describe its shape: ellipse major and minor axis length (L_1 and L_2, i.e., length and width, respectively) and the least-squares circle radius (r). Left scapulas were transformed as right scapulas to homogenise data.

2.5 | Statistical analysis

Based on the previously established dataset, the reliability of the ArUco-based localisation stylus to digitalise cartilage contours was assessed. Intra-observer repeatability and inter-observer reproducibility were computed using an ICC (Mokkink et al., 2016), respectively, ICC_{intra} and ICC_{inter}. Intra-observer repeatability represents in this study the degree of agreement between the results obtained by
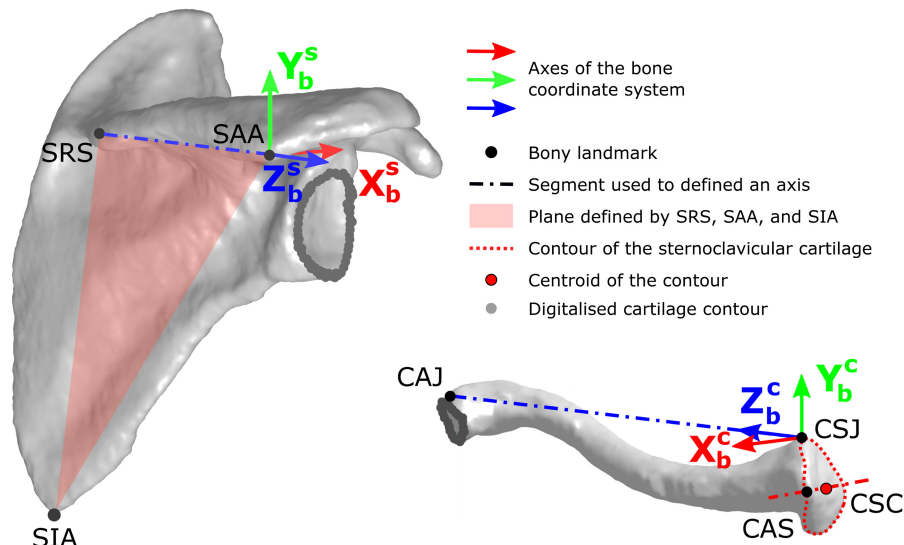
FIGURE 2 Illustration of the position and orientation of the digitalised cartilage contours. The position and orientation of digitalised cartilage contours are illustrated in relation to the related for a right scapula and clavicle. The geometrical elements used to define bone coordinate system axes are also reported: SAA: origin of the scapula coordinate system, Z_s^b: The line connecting SRS and SAA, pointing to SAA, X_s^b: The line perpendicular to the plane formed by SIA, SAA, and SRS, pointing forward. Y_s^b: The common line perpendicular to X_s^b and Z_s^b, pointing upward; CSJ: origin of the clavicle coordinate system, Z_c^b: The line connecting CSJ and CAJ, pointing to CAJ, X_c^b: The line connecting CAS to CSC, i.e., the centre of the sternoclavicular cartilage, pointing forward, Y_c^b: The common line perpendicular to X_c^b and Z_c^b, pointing upward.

the same examiner across the three consecutive digitalisations of each cartilage contour. Inter-observer repeatability represents the degree of agreement among the three examiners during digitalisation of each cartilage contour. A single measure, two-way, mixed model-type absolute ICC coefficients were used, that is, ICC(3,k) (Shrout & Fleiss, 1979). Variance components were estimated first with the *lme4* package (1.1–28) (R-Core-Team, 2020b). The total variance was defined as the class component variance sum:

$$\sigma_{total}^2 = \sigma_{cartilage}^2 + \sigma_{operator}^2 + \sigma_{digitalisation}^2 + \sigma_{residual}^2 \quad (1)$$

where $\sigma_{cartilage}^2$, $\sigma_{examiner}^2$, $\sigma_{digitalisation}^2$, and $\sigma_{residual}^2$ are, respectively, the cartilage, the examiner, the digitalisation, and the residual variance. Following the methodology proposed by Chia and Sangeux (2017), ICC estimates were then obtained as follows:

$$ICC_{intra} = \frac{\sigma_{total}^2 - \left(\sigma_{digitalisation}^2 + \sigma_{residual}^2\right)}{\sigma_{total}^2} \quad (2)$$

$$ICC_{inter} = \frac{\sigma_{total}^2 - \left(\sigma_{operator}^2 + \sigma_{residual}^2\right)}{\sigma_{total}^2} \quad (3)$$

ICC estimates were qualified as relative reliability metrics and classified as poor (<0.5), moderate (0.5 to 0.75), good (0.75 to 0.90), and excellent (≥0.90) agreement (Koo & Li, 2016).

Standard error of measurement (SEM) was also quantified both for intra-observer repeatability and inter-observer reproducibility as an absolute reliability metric and computed as follows:

$$SEM_{intra} = \sqrt{\sigma_{total}^2 \times \left(1 - ICC_{intra}\right)} \quad (4)$$

$$SEM_{inter} = \sqrt{\sigma_{total}^2 \times \left(1 - ICC_{inter}\right)} \quad (5)$$

As each SEM value is related to a specific range and unit of measurement, %SEM was additionally calculated to aid interpretation. A classification criterion of acceptability was arbitrarily defined for each unit: excellent (<1 mm or °), good (1 mm or ° to 2 mm or °), moderate (2 mm or ° to 3 mm or °), and poor (3 mm or ° or higher).

The mean inter and intra-observer 95% CI was computed as ±1.96 SEM (Mokkink et al., 2010). All computations related to the reliability analysis were performed in R 4.1.2 and RStudio (version 2021.09.0 build 351) (R-Core-Team, 2018).

3 | RESULTS

Mean, standard deviation, confidence interval, and results of the statistical analysis are reported in Table 2 for the glenoid cartilage related to the glenohumeral joint and in Table 3 for the clavicle cartilage related to the acromioclavicular joint. Overall, 35.2 ± 2.4 s and 26.6 ± 10.2 s were required by each examiner to digitalise the contour of a glenoid cartilage and an acromioclavicular cartilage, respectively.

Concerning the glenoid cartilage (Table 2), the intra-observer relative reproducibility always demonstrated good-to-excellent agreement, with the ICC ranging between 0.89 and 1.00,
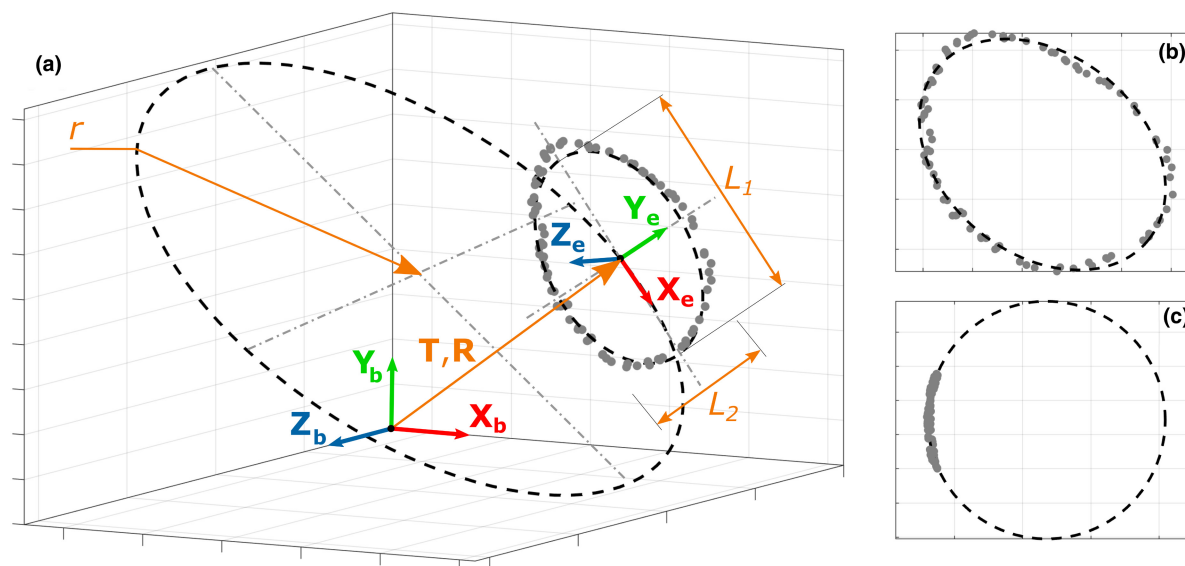
FIGURE 3 Parametrisation of a measured 3D point cloud defining a cartilage contour. (a) 3D point cloud (grey points), coordinate systems (bone coordinate system: X_b, Y_b, Z_b, ellipse coordinate system: X_e, Y_e, Z_e) and related parameters (**T**: $X_{cart}, Y_{cart}, Z_{cart}$ – 3D position of the ellipse in the bone coordinate system, **R**: $\alpha_{cart}, \beta_{cart}, \gamma_{cart}$ – 3D orientation of the ellipse in the bone coordinate system, L_1 – length of the ellipse major axis, L_2 – length of the ellipse minor axis, and r – radius of the least-squares circle). (b) Orthogonal projection of the 3D point cloud on its least-squares plane and fitting with an ellipse using a least-squares approach based on orthogonal distance. (c) Orthogonal projection of the 3D point cloud on a plane having a normal vector along the minor axis of the previously defined ellipse and fitting with a least-squares circle.

TABLE 2 Mean, standard deviation, confidence interval, ICC, and standard error of measurement observed for the glenoid cartilage related to the glenohumeral joint.

					Intra-observer		Inter-observer	
Parameter	**Unit**	**Mean**	**Std**	**95% CI**	**ICC**	**SEM (SEM%)**	**ICC**	**SEM (SEM%)**
X_{cart}	mm	31.8	3.1	31.1; 32.5	0.89‡	1.1 (3.6)‡	0.85‡	1.3 (4.1)‡
Y_{cart}	mm	−17.7	3.4	−18.4; −16.9	0.95†	1.0 (5.7)‡	0.71*	2.3 (13.6)*
Z_{cart}	mm	−16.6	6.6	−18.0; −15.1	1.00†	0.4 (2.4)†	0.99†	0.6 (3.3)†
α_{cart}	deg	0.9	6.2	−0.5; 2.3	0.98†	0.9 (4.4)†	0.97†	1.1 (5.3)‡
β_{cart}	deg	10.4	3.4	9.6; 11.1	0.92†	1.1 (10.2)‡	0.91†	1.2 (11.0)‡
γ_{cart}	deg	−93.8	6.6	−95.3; −92.4	0.95†	1.7 (1.8)‡	0.93†	1.9 (2.1)‡
L_1	mm	28.8	1.1	28.6; 29.0	0.92†	0.2 (1.1)†	0.77‡	0.3 (1.9)†
L_2	mm	20.4	1.2	20.2; 20.7	0.96†	0.1 (1.1)†	0.89‡	0.2 (1.8)†
r	mm	38.1	5.5	36.9; 39.4	0.68*	3.0 (7.9)*	0.64*	3.2 (8.4)

Note: **Parameters:** 3D position of the ellipse $X_{cart}, Y_{cart}, Z_{cart}$, 3D orientation of the ellipse $\alpha_{cart}, \beta_{cart}, \gamma_{cart}$, length of the ellipse major axis L_1, length of the ellipse minor axis L_2, and radius of the least-squares circle r. **Classification:** †excellent (in blue); ‡good (in green); *moderate (in orange); poor (black).

Abbreviations: CI 95%, 95% confidence interval; ICC, intra-class correlation; SEM, standard error of measurement; Std, standard deviation.

associated with good-to-excellent SEM values, except for the radius of the least-squares circle (ICC = 0.68, SEM = 3.0 mm). For this parameter, the mean intra-observer 95% CI of the mean was 5.9 mm. The inter-observer relative reproducibility generally demonstrated good-to-excellent agreement, with the ICC ranging between 0.77 and 0.99, associated with good-to-excellent SEM values. Only the cartilage position along the inferior–superior Y_s^b axis (ICC = 0.71, SEM = 2.3 mm) and the least-squares circle radius

(ICC = 0.64, SEM = 3.2 mm) demonstrated poorer results. For these two parameters, the mean intra-observer 95% CI of the mean was 4.5 and 5.2 mm, respectively.

Concerning the clavicle cartilage (Table 3), the intra-observer relative reproducibility always demonstrated good-to-excellent agreement, with the ICC ranging between 0.81 and 0.99. However, the cartilage orientation around the medial-lateral Z_b^s axis (ICC = 0.81, SEM = 4.9°) and the least-squares circle radius

TABLE 3 Mean, standard deviation, confidence interval, ICC, and standard error of measurement observed for the clavicle cartilage related to the acromioclavicular joint.

Parameter	Unit	Mean	Std	95% CI	Intra-observer		Inter-observer	
					ICC	SEM (SEM%)	ICC	SEM (SEM%)
X_{cart}	mm	0.1	2.7	−0.5; 0.6	0.90[†]	0.9 (9.0)[†]	0.67[*]	1.6 (16.3)[‡]
Y_{cart}	mm	−6.9	1.4	−7.2; −6.6	0.81[‡]	0.6 (8.8)[†]	0.75[‡]	0.7 (10.2)[†]
Z_{cart}	mm	134.9	7.9	133.3; 136.6	0.99[†]	0.7 (0.5)[†]	0.97[†]	1.4 (1.0)[‡]
α_{cart}	deg	21.9	13.8	19.0; 24.8	0.98[†]	2.0 (6.2)[‡]	0.94[†]	3.2 (10.0)
β_{cart}	deg	39.0	11.6	36.6; 41.4	0.99[†]	1.1 (2.9)[‡]	0.98[†]	1.7 (4.4)[‡]
γ_{cart}	deg	−6.0	12.5	−8.6; −3.3	0.81[‡]	4.9 (11.1)	0.81[‡]	4.9 (11.1)
L_1	mm	20.4	3.2	19.7; 21.0	0.98[†]	0.3 (2.5)[†]	0.93[†]	0.5 (4.5)[†]
L_2	mm	13.0	1.2	12.7; 13.2	0.92[†]	0.2 (2.6)[†]	0.78[‡]	0.3 (4.3)[†]
r	mm	18.3	9.9	16.2; 20.4	0.93[†]	2.8 (15.4)[*]	0.73[*]	5.4 (29.6)

Note: **Parameters:** 3D position of the ellipse X_{cart}, Y_{cart}, Z_{cart}, 3D orientation of the ellipse α_{cart}, β_{cart}, γ_{cart}, length of the ellipse major axis L_1, length of the ellipse minor axis L_2, and radius of the least-squares circle r. **Classification:** [†]excellent (in blue); [‡]good (in green); [*]moderate (in orange).
Abbreviations: CI 95%, 95% confidence interval; ICC, intra-class correlation; SEM, standard error of measurement; Std, standard deviation.

(ICC = 0.93, SEM = 2.8 mm) demonstrated poorer absolute reproducibility results. The inter-observer relative reproducibility generally demonstrated good-to-excellent agreement, with the ICC ranging between 0.75 and 0.98. The cartilage position along the antero-posterior X_c^b (ICC = 0.67, moderate agreement) and the least-squares circle radius (ICC = 0.73, moderate agreement) demonstrated poorer results. For these two parameters, the mean intra-observer 95% CI of the mean was 3.1 mm and 10.6 mm, respectively. Furthermore, the cartilage orientation around the anterior–posterior X_s^b (ICC = 0.94, SEM = 3.2°) and the medial–lateral Z_s^b (ICC = 0.81, SEM = 4.9°) axes demonstrated poorer absolute reproducibility results.

4 | DISCUSSION

Various 3D scanning systems are available to digitalise anatomical structures (Govender et al., 2023; Sindhu & Soundarapandian, 2019). This study was focused on a manual tactile contact method based on a hand-held stylus made of ArUco markers (Garrido-Jurado et al., 2014; Wu et al., 2017). In particular, the reliability of this simple approach was assessed during the 3D digitalisation of shoulder cartilage contours.

The proposed parameters describing cartilage contours allow for shape analysis of these structures. Concerning the glenoid cartilage, its mean length and width, i.e., the articular surface of the glenoid fossa excluding the labrum, were, respectively, 28.8 ± 1.2 and 20.4 ± 1.2 mm. These dimensions are consistent with the mean glenoid cartilage shape measured by Hata et al. (1992) (length: 33.5 ± 4.1 mm, width: 26.5 ± 3.2 mm) on a larger population (N = 31 shoulders). The 3D radius of curvature was 38.1 ± 5.5 mm, which is also consistent with previous measurements. Indeed, McPherson et al. measured on 93 shoulders a mean glenoid radius of curvature

of 32.2 ± 7.6 and 40.6 ± 14 mm in antero-posterior and axillary–lateral views, respectively (Mcpherson et al., 1997). To the best of our knowledge, the glenoid cartilage position related to a scapula coordinate system is rarely reported in the literature. Furthermore, the glenoid cartilage orientation, in particular glenoid version and inclination, is still commonly measured in 2D based on radiographs (Mansat & Bonnevialle, 2013) and cannot be directly compared to the presents results expressed in the scapula ISB coordinate system. Concerning the acromioclavicular cartilage, its mean length and width were, respectively, 20.4 ± 3.2 and 13.0 ± 1.2 mm. These dimensions are consistent with the mean shape measured by Nakazawa et al. (2016) (length: 20.5 [17; 33] mm, width: 8.2 [5; 13] mm) on the external third of the clavicle bone using CT scan (N = 10 shoulders) (Nourissat et al., 2007). The 3D radius of curvature was 18.3 ± 9.9 mm. This was the shape parameter most affected by variability. This can be explained by the various morphologies of the acromioclavicular joint reported in the literature, defining various joint curvatures (Colegate-Stone et al., 2010). As for the glenoid cartilage, comparison of the acromioclavicular cartilage position and orientation in a clavicle coordinate system is made difficult by the use of various coordinate systems or because of data scarcity.

The present results generally demonstrate a good-to-excellent inter and intra-observer reliability both on medium-size (glenoid cartilage) and small-size (acromioclavicular cartilage) cartilage contours. This supports the fact that hand-held stylus can be valuable tools for 3D digitalisation, as previously demonstrated on knee ligaments (Athwal et al., 2020). In particular, such a digitalisation is often performed after dissection, which can allow visual identification of surrounding anatomical structures. However, as being guided by the operator's vision, this approach can lead to several discrepancies when the targeted structure is not well-recognisable. Hence, it appeared that the inferior–superior limits of the glenoid cartilage were more difficult to identify in a reliable way, as well as

the antero-posterior limits of the clavicle cartilage. Unsurprisingly, cartilage borders in these directions are more prone to identification error due to other surrounding structures. Indeed, a fibrocartilaginous transition area between the glenoid cartilage and the labrum fibrous tissue in the superior and inferior parts of the glenoid is frequently observed (Cooper et al., 1992). Similarly, the anterior and posterior parts of the clavicle distal end correspond to ligament insertions and sometimes to a degenerated acromioclavicular disk (Nakazawa et al., 2016). It must also be noted that, even with a relative reliability being good to excellent, acromioclavicular cartilage orientation around the anterior–posterior and the medial–lateral axes demonstrated poor absolute reliability, with SEM values at 3.2° and 4.9°, respectively. Depending on the application, these levels might limit the capacity of the approach to provide reliable orientations in small structures such as the acromioclavicular cartilage.

This study has some limitations. First, due to the mean age of the specimens (77.4 ± 9.99 years), cartilage morphologic changes may have appeared due to various progression of osteoarthritis (Pritzker et al., 2006) potentially affecting identification of cartilage surfaces. Still, the present results suggest that a good-to-excellent agreement can be obtained in such conditions. Second, as the digitalisation process presented in this study is guided by vision, the operator's knowledge and experience is directly related to the reported results. In this sense, the present results are not directly generalisable, justifying the choice for the use of a single measure, two-way mixed model ICC(3,k). Still, as the three operators presented very different backgrounds (F.M. – biomechanical researcher, C.E.K – instrumentation engineer, and P.R. – intern in orthopaedic trauma surgery), the reported levels of reproducibility are encouraging, while further research will be required to demonstrate the clinical applicability. Third, following the ISB recommendations, the x-axis of the clavicle should be defined perpendicular to the z-axis of the clavicle and the y-axis of the thorax (Wu et al., 2005). As the thorax was not available is this study, another approach has been used to define the clavicle coordinate system (Gutierrez Delgado et al., 2017). It results that a rotational offset around the clavicle medial–lateral axis may appear between the approach used in this study and ISB recommendations. Fourth, the parameter set used to describe the cartilage position, orientation, and shape might not be adaptable to every cartilage type. In particular, some cartilages are flatter than others (Emura et al., 2014), leading to discrepancies when trying to fit a sphere to estimate their curvature. This may explain the moderate reproducibility results obtained on the curvature r parameter for both analysed cartilages. This could be improved by defining a curvature threshold allowing to discriminate flat cartilages.

5 | CONCLUSION

The use of an ArUco-based localisation stylus can thus be a reliable and accurate (Le et al., 2022) approach to digitalise anatomical structures such as shoulder cartilage contours. Furthermore, it represents a fast and cost-effective approach in constrast to the current gold standard, that is, MRI (Hayashi et al., 2011), known as being costly and time-consuming. Still, further research is required to compare the two approaches.

ORCID

Florent Moissenet https://orcid.org/0000-0001-6479-1911
Christian Elmo Kulanesan https://orcid.org/0000-0002-3875-1980

REFERENCES

Athwal, K.K., Willinger, L., Shinohara, S., Ball, S., Williams, A. & Amis, A.A. (2020) The bone attachments of the medial collateral and posterior

oblique ligaments are defined anatomically and radiographically. *Knee Surgery, Sports Traumatology, Arthroscopy*, 28, 3709–3719.

Chia, K. & Sangeux, M. (2017) Quantifying sources of variability in gait analysis. *Gait & Posture*, 56, 68–75.

Colegate-Stone, T., Allom, R., Singh, R., Elias, D.A., Standring, S. & Sinha, J. (2010) Classification of the morphology of the acromioclavicular joint using cadaveric and radiological analysis. *The Journal of Bone & Joint Surgery British*, 92-B, 743–746.

Cooper, D.E., Arnoczky, S.P., O'brien, S.J., Warren, R.F., Dicarlo, E. & Allen, A.A. (1992) Anatomy, histology, and vascularity of the glenoid labrum. An anatomical study. *The Journal of Bone and Joint Surgery. American Volume*, 74, 46–52.

Dingler, S. (2021) Fitting ellipses to noisy measurements. *arXiv*.

Elmo Kulanesan, C. (2023) *Navigation en temps réel pour chirurgie opératoire de l'épaule par fusion de données* (Doctoral thesis). Université Savoie Mont Blanc.

Emura, K., Arakawa, T., Miki, A. & Terashima, T. (2014) Anatomical observations of the human acromioclavicular joint. *Clinical Anatomy*, 27, 1046–1052.

Garrido-Jurado, S., Muñoz-Salinas, R., Madrid-Cuevas, F.J. & Marín-Jiménez, M.J. (2014) Automatic generation and detection of highly reliable fiducial markers under occlusion. *Pattern Recognition*, 47, 2280–2292.

Govender, S., Cronjé, J.Y., Keough, N., Oberholster, A.J., Van Schoor, A.N., de Jager, E.J. et al. (2023) Emerging imaging techniques in anatomy: For teaching, research and clinical practice. In: Shapiro, L. & Rea, P.M. (Eds.) *Biomedical visualisation: Volume 13 – the art, philosophy and science of observation and imaging*. Cham: Springer International Publishing.

Gutierrez Delgado, G., De Beule, M., Ortega Cardentey, D.R., Segers, P., Iznaga Benítez, A.M., Rodríguez Moliner, T. et al. (2017) Procedure to describe clavicular motion. *Journal of Shoulder and Elbow Surgery*, 26, 490–496.

Haleem, A. & Javaid, M. (2019) 3D scanning applications in medical field: A literature-based review. *Clinical Epidemiology and Global Health*, 7, 199–210.

Hargett, Z., Gutierrez, M. & Harman, M. (2020) Verification of manual digitization methods during experimental simulation of knee motion. *Journal of Verification, Validation and Uncertainty Quantification*, 5, 031004.

Hata, Y., Nakatsuchi, Y., Saitoh, S., Hosaka, M. & Uchiyama, S. (1992) Anatomic study of the glenoid labrum. *Journal of Shoulder and Elbow Surgery*, 1, 207–214.

Hayashi, D., Guermazi, A., Crema, M.D. & Roemer, F.W. (2011) Imaging in osteoarthritis: What have we learned and where are we going? *Minerva Medica*, 102, 15–32.

Koo, T.K. & Li, M.Y. (2016) A guideline of selecting and reporting Intraclass correlation coefficients for reliability research. *Journal of Chiropractic Medicine*, 15, 155–163.

Le, T.S., Tran, Q.V., Nguyen, X.L. & Lin, C.Y. (2022) Solpen: An accurate 6-DOF positioning tool for vision-guided robotics. *Electronics*, 11, 618.

Mansat, P. & Bonnevialle, N. (2013) Morphology of the normal and arthritic glenoid. *European Journal of Orthopaedic Surgery & Traumatology*, 23, 287–299.

Mcpherson, E.J., Friedman, R.J., An, Y.H., Chokesi, R. & Dooley, R.L. (1997) Anthropometric study of normal glenohumeral relationships. *Journal of Shoulder and Elbow Surgery*, 6, 105–112.

Moissenet, F., Rastoll, C., Gonzalez, D., Foukia, N., Lauria, M., Armand, S. et al. (2022) Validation of a robotic testing procedure for shoulder in-vitro biomechanical testing. *World Journal of Surgery and Surgical Research*, 5, 1392.

Mokkink, L.B., Prinsen, C.A.C., Bouter, L.M., Vet, H.C.W.D. & Terwee, C.B. (2016) The COnsensus-based standards for the selection of health measurement INstruments (COSMIN) and how to select an outcome measurement instrument. *Brazilian Journal of Physical Therapy*, 20, 105–113.

Mokkink, L.B., Terwee, C.B., Patrick, D.L., Alonso, J., Stratford, P.W., Knol, D.L. et al. (2010) The COSMIN checklist for assessing the methodological quality of studies on measurement properties of health status measurement instruments: An international Delphi study. *Quality of Life Research*, 19, 539–549.

Nakazawa, M., Nimura, A., Mochizuki, T., Koizumi, M., Sato, T. & Akita, K. (2016) The orientation and variation of the acromioclavicular ligament: An anatomic study. *The American Journal of Sports Medicine*, 44, 2690–2695.

Nourissat, G., Henon, A., Debet-Mejean, A., Clement, P., Dumontier, C., Sautet, A. et al. (2007) Three-dimensional computed tomographic scan of the external third of the clavicle. *Arthroscopy: The Journal of Arthroscopic & Related Surgery*, 23, 29–33.

Pritzker, K.P.H., Gay, S., Jimenez, S.A., Ostergaard, K., Pelletier, J.P., Revell, P.A. et al. (2006) Osteoarthritis cartilage histopathology: Grading and staging. *Osteoarthritis and Cartilage*, 14, 13–29.

R-Core-Team. (2018) *R: A language and environment for statistical computing. R Foundation for Statistical Computing* [Online]. https://www.R-project.org/

R-Core-Team. (2020a) *ICC.Sample.Size: Calculation of sample size and power for ICC* [Online]. https://www.rdocumentation.org/packages/ICC.Sample.Size/versions/1.0/topics/ICC.Sample.Size-package

R-Core-Team. (2020b) *lmer: Fit linear mixed-effects models* [Online]. https://www.rdocumentation.org/packages/lmerTest/versions/3.1-3/topics/lmer

Schweighofer, G. & Pinz, A. (2006) Robust pose estimation from a planar target. *IEEE Transactions on Pattern Analysis and Machine Intelligence*, 28, 2024–2030.

Shrout, P.E. & Fleiss, J.L. (1979) Intraclass correlations: Uses in assessing rater reliability. *Psychological Bulletin*, 86, 420–428.

Sindhu, V. & Soundarapandian, S. (2019) Three-dimensional modelling of femur bone using various scanning systems for modelling of knee implant and virtual aid of surgical planning. *Measurement*, 141, 190–208.

Sood, A., Dogra, V. & Pathmanathan, G. (2021) 3D surface digitization in scientific research and product development. *Forensic Medicine and Anatomy Research*, 09, 11–23.

Van Sint Jan, S. (2007) *Color atlas of skeletal landmark definitions: Guidelines for reproducible manual and virtual palpations*. Edinburgh, New York: Churchill Livingstone/Elsevier.

Wu, G., Van Der Helm, F.C.T., Veeger, H.E.J., Makhsous, M., Van Roy, P., Anglin, C. et al. (2005) ISB recommendation on definitions of joint coordinate systems of various joints for the reporting of human joint motion—part II: Shoulder, elbow, wrist and hand. *Journal of Biomechanics*, 38, 981–992.

Wu, P.C., Wang, R., Kin, K., Twigg, C., Han, S., Yang, M.H. et al. (2017) DodecaPen: Accurate 6DoF tracking of a passive stylus. *The 30th Annual ACM Symposium*. (vol. 17, pp. 365–374).